The Color of Lactotroph Secretory Granules Stained with FM1-43 Depends on Dye Concentration

Joseph M. Johnson and William J. Betz
Department of Physiology and Biophysics, University of Colorado Medical School, Aurora, Colorado 80045

ABSTRACT When pituitary lactotroph granules undergo exocytosis in the presence of FM1-43, their cores absorb dye and fluoresce brightly. We report that different granules fluoresce with different colors, despite being stained with a single fluorescent dye; emission spectra from individual granules show up to a 25 nm difference between the greenest and reddest granules. We found a correlation between granule color and average fluorescence intensity, suggesting that granule color depends upon dye concentration. We confirmed this in two ways: by increasing FM dye concentration in granules, which red shifted granule color, and by partially photobleaching the FM dye in granules, which green shifted granule color. Increasing stimulation intensity (by increasing KCl concentration) increased the proportion of red granules, indicating that granules exocytosing during intense stimulation bound more dye. This, perhaps, reflects differences in granule core maturation and condensation in which mature granules with condensed cores bind more FM dye but require more intense stimulation to be released. Concentration-dependent color shifts of FM dyes may be useful for monitoring aggregation processes occurring on a size scale smaller than the optical limit.

INTRODUCTION

Lactotroph cells from the anterior pituitary secrete the hormone prolactin (PRL), an ~22 kD protein that is stored in and released from dense core granules (1). Individual exocytic events can be optically monitored in cultured lactotrophs using the fluorescent dye FM1-43, a styryl dye that has been used extensively to monitor vesicle cycling in both neurons and neuroendocrine cells (2). FM1-43 is an amphipathic molecule that is water soluble but reversibly partitions into hydrophobic interfaces, increasing in quantum yield by approximately two orders of magnitude in the process. Both the dense core and the membrane of a lactotroph granule are stained with FM1-43, causing bright staining of the entire granule. Moreover, FM dye-binding components of the core are retained after exocytosis and are retrieved by subsequent endocytosis. Endocytosis occurs slowly in lactotrophs, as evidenced by the ability to wash out FM dye from granule cores 10–20 min after exocytosis (3). During intense stimulation, multiple granules can exocytose through a single fusion pore by undergoing granule-granule fusion, a process termed ''compound exocytosis'' (4).

We report here that not all lactotroph granules stained with FM1-43 fluoresce with the same color, although only one type of fluorophore is present (Fig. 1; Supplementary Material, Movie S1). We find that the greenest granules fluoresce with an emission peak around 570 nm and the reddest granules fluoresce with a peak near 595 nm. We use the terms red and green in a relative sense, and in an absolute sense the emission peak of green granules corresponds to the color yellow and red granules corresponds to orange (5).

We demonstrate that different colors are caused by different concentrations of FM dye within each granule. We also report a red shift of granule color with increasing KCl concentration, used to stimulate exocytosis in lactotrophs. We propose that differently colored granules are due to differences in the density of granule cores, with more dense cores taking up more FM dye, and that less dense granules exocytose preferentially with mild stimulation. Our results correlate with a granule maturation process that has been previously described in lactotrophs in which granules become more dense and less readily exocytic as they age (6,7). Some aspects of this work have been preliminarily presented (8).

MATERIALS AND METHODS

Materials

Sprague-Dawley rats were purchased from Charles River Laboratories (Wilmington, MA). FM1-43 was purchased from Molecular Probes/Invitrogen (Eugene, OR). Media was purchased from Invitrogen (Carlsbad, CA). Buffer components, phorbol 12-myristate 13-acetate (PMA), forskolin, and 3-isobutyl-1-methylxanthine (IBMX) were purchased from Sigma-Aldrich (St. Louis, MO). Phosphatidylcholine from egg yolk (egg PC) was purchased from Avanti Polar Lipids (Alabaster, AL). Affinity purified PRL was purchased from Dr. A. F. Parlow of the National Hormone and Peptide Program (Harbor-UCLA Medical Center, Los Angeles, CA).

Cell culture

Primary cultures of lactotroph cells were prepared following the protocol from Angleson et al. (3). Briefly, anterior pituitary cells were obtained from male Sprague-Dawley rats between 250–350 g by enzymatic dispersion

Submitted May 10, 2007, and accepted for publication November 15, 2007.

Address reprint requests to William J. Betz, University of Colorado Medical School, Dept. of Physiology, University of Colorado Health Sciences Center, RC-1 North Tower, P18-7129, PO Box 6511, Mail Stop F8307, Aurora, CO 80045. Tel.: 303-742-4502; E-mail: bill.betz@uchsc.edu.

Joseph M. Johnson's present address is Dept. of Physiology and Biophysics, University of Southern California, Los Angeles, CA 90089.

Editor: Robert Hsiu-Ping Chow.

0006-3495/08/04/3167/11 $2.00

doi: 10.1529/biophysj.107.112573

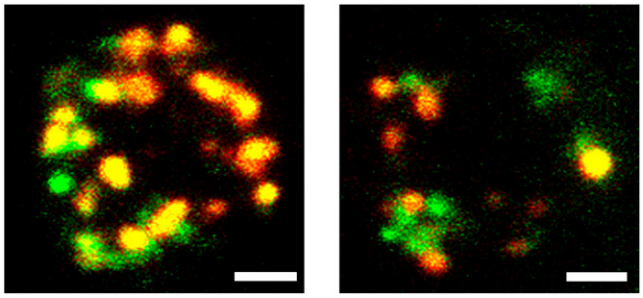

FIGURE 1 Lactotrophs stained with FM1-43 show granules of different colors. We show two examples of lactotrophs imaged through fluorescein (*green*) and tetramethylrhodamine (*red*) filter sets using a confocal microscope in which all confocal planes have been collapsed into one image. Scale bars = 2 μm. See also Movie S1.

followed by separation on a Percoll gradient. Cells were plated on polylysine-coated coverslips and cultured for 2–3 days before experiments. Cultured cells were ~50% lactotroph as estimated by immunostaining for PRL, which is consistent with previously reported values (3). Culture dishes were maintained at 33°C–35°C during imaging (except, as noted, for imaging cells in two colors and imaging cells during stimulation), and images were acquired within 20–60 min after staining.

Standard loading protocol

Lactotrophs were stained with FM1-43 by stimulating exocytosis with a high $[K^+]$ solution in the presence of 4 μM FM dye for 2 min, then incubating lactotrophs in a low $[K^+]$ solution in the presence of 4 μM FM dye for an additional 18 min. This allowed enough time for endocytosis to occur, after which FM dye could be washed from solution and be retained in granule cores (3). The standard low $[K^+]$ solution contained (in mM): 140 NaCl, 5 KCl, 1 $MgCl_2$, 10 glucose, 10 HEPES, and 8 $CaCl_2$. The high $[K^+]$ solution was the same composition except it contained 100 mM KCl and 45 mM NaCl. To examine the effects of dye concentration, FM1-43 concentration was varied from 1 to 30 μM. To examine the effects of stimulation intensity, KCl concentration was varied from 5 to 100 mM, replacing equivalent amounts of NaCl. All loading protocols were performed at 37°C.

Imaging cells in two colors

Following the standard loading protocol, the cells in Fig. 1 were imaged on an Olympus (Tokyo, Japan) spinning disk confocal with a 100×, 1.35 numerical aperture (NA) objective, collecting 0.5 μm slices. Samples were excited with a mercury arc lamp, and emission was detected in two colors by switching between two excitation/emission filter sets (green excitation 470/20 nm, green emission 520/40 nm, red excitation 545/20 nm, and red emission 600/55 nm). The time lag between acquisition of red and green images was <0.5 s. These images were collected at room temperature. We chose to display the images in Fig. 1 with green and red pseudocolors because they were acquired through fluorescein and rhodamine optical filter sets. Researchers will typically view FM1-43-stained samples through these two filter sets and may observe the same type of inhomogeneities in sample color that Fig. 1 displays.

Measuring the spectra of lactotroph granules

Following the standard loading protocol, lactotrophs were imaged on a Zeiss LSM-510 Meta scanning confocal microscope (Zeiss, Thornwood, NY) using a 63×, 0.9 NA objective, collecting 0.5 μm slices. Samples were excited with an Ar ion laser (488 nm), and identical settings were used for all experiments (1% laser transmission) except when FM dye concentration was varied (where laser transmission was adjusted from 0.25% to 2%—granule intensity values reported for these experiments were adjusted for varying laser transmissions). Using the Meta attachment, fluorescence was detected in eight channels (with 10.7 nm bandwidth) centered at 543, 554, 564, 575, 586, 596, 607, and 618 nm. The spectral response of the Meta was stable at all signal levels, as determined by measuring the spectra of 5 μM rhodamine 6G (R6G) at a variety of laser powers (0.1%–10% transmission).

Image and data analysis

Images were exported in TIFF (tagged image file format) format and image analysis was performed in a custom-written MATLAB program (MathWorks, Natick, MA) that allowed automated spot picking in three dimensions (3D). Stacks were processed for spot picking by averaging the intensities from all eight channels, smoothing the images (Gaussian weighting, 7 pix radius, standard deviation 0.65), and subtracting an average background intensity. Spots were identified using the MATLAB watershed function, which segmented the processed stack into regions by identifying minimum intensity contours. To make regions more spherical, pixels with intensities <20% of the brightest pixel in the region were discarded. Spots with fewer than 40 or more than 10,000 pixels were discarded.

Confocal slices of an FM1-43-stained lactotroph with autopicked spots are shown in Fig. 2 and Movie S2. In Fig. 2 some spots appear to have not been picked in certain confocal slices (e.g., *panel* ''3 μm''); however, these spots were picked in subsequent confocal slices (e.g., *panel* ''4 μm''). This is due to discarding pixels of <20% intensity, which may cause a slight underestimation of the size of bright spots compared to dim spots. Spot sizes were obtained from processed images; however, intensity values (in eight channels) were obtained from unprocessed images. The accuracy of the automated analysis was tested by hand picking spots for a subset of images. The automated analysis was accurate with the exception that spot diameters were overestimated by 20% on average compared to manually measuring spots.

For data analysis of individual spots, an average background intensity was subtracted. The autofluorescence of spots in the absence of FM1-43 was too dim to measure and was therefore not expected to significantly affect granule color. Spectral variations in the microscope were corrected by comparing to spectra of 5 μM rhodamine 6G in solution (R6G) measured on the Zeiss Meta. A correction factor for each channel was defined by dividing the measured R6G spectrum by a standard R6G spectrum (measured on a corrected fluorescence spectrometer), and the spot spectra were then divided by the correction factor. Granule intensity was quantified using the average

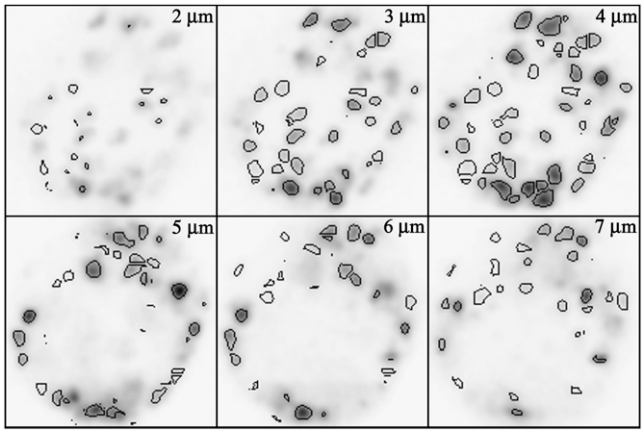

FIGURE 2 Spots can be identified in 3D using automated image analysis software. We show six confocal slices, beginning 2 μm above the coverslip and spaced 1 μm apart, of a lactotroph with FM1-43-stained granules. Images are displayed in negative for clarity. Black lines around each granule delineate spots identified with our automated spot picking algorithm. Each image is 11 × 11 μm. Also see Movie S2.

intensity, which equaled the summed intensity of all eight channels averaged over all of the pixels within a spot. For each spot a red/green ratio (R/G) was defined, where R/G = summed intensity of the four reddest channels divided by the summed intensity of the four greenest channels. This allowed quantification of spot color. As an alternative method for quantifying color, individual granule spectra from Fig. 3 were fit with Gaussians, and the Gaussian peak was reported as the peak wavelength of the spectra. Gaussian fits were carried out in a custom-written MATLAB program, and the goodness-of-fit was evaluated using the square of the correlation coefficient (R^2). Errors reported represent standard error, and all significant differences were determined using Student's *t*-test.

Photobleaching FM1-43-stained lactotroph granules

Following the standard loading protocol, cells were imaged on the Zeiss Meta. A single confocal image was collected at the equatorial plane of a cell before and after photobleaching with 100% laser transmission. Spots were identified using the automated spot finding algorithm, and the color was compared for the same spots before and after photobleaching. Dim spots showed a significant scatter in R/G values (probably due to being mostly out of the focal plane), and these were not included in the ΔR/G analysis (see Fig. S1).

Imaging cells during stimulation

The kinetics of granule staining was obtained by stimulating lactotrophs in the presence of 4 μM FM1-43 while imaging on the Zeiss LSM. Cells were stimulated by applying a high [K^+] buffer (either 50 mM or 100 mM KCl) with a microaspirator for 30 s, starting 5 s after the start of imaging. Granule fluorescence was imaged in the wavelength region of 591–709 nm, with a frame duration of 247 ms. Cells were maintained at room temperature during imaging.

Measurement of FM1-43 spectra in solution

Egg PC vesicles of 100 nm diameter (1 mM) were prepared in a Ca^{2+}-free low [K^+] solution according to previous protocols (9). PRL (12 μM) was dissolved in a low [K^+] solution. The fluorescence spectrum was measured of 1, 3, 10, and 30 μM FM1-43 bound to egg PC vesicles or PRL in solution, using a fluorescence spectrometer. FM1-43 fluorescence was excited at 475 nm. Spectra were corrected by comparing to a spectrum of 5 μM R6G. A 12 μM PRL solution was used for solution measurements, which bound only a fraction of the total amount of FM1-43 at each concentration (~20%). FM1-43 has a small, but measurable fluorescence in aqueous solution, which is red shifted compared to bound FM1-43. The fluorescence from unbound FM1-43 caused a 4–5 nm, artifactual red shift of the emission peak of PRL-bound FM1-43. To correct for this red shift, spectra of FM1-43 bound to PRL were background corrected by subtracting spectra of the same concentration of FM1-43 without PRL. No change in the emission peak of FM1-43 was noted for varying PRL concentrations, once the background due to unbound FM1-43 was subtracted (data not shown). The fluorescence contribution of PRL itself should be negligible at the wavelengths examined. Because an excess of egg PC was used (1 mM) the majority of FM1-43 was bound, and so these spectra were background corrected by subtracting a spectrum of 1 mM egg PC with no FM1-43. For further details about FM1-43 solution spectra, methods for estimating the amount of FM1-43 bound and background correction methods, see Fig. S2.

Drug preparations

PMA (100 nM) or forskolin (10 μM) was applied for 10 min before and during stimulation with high [K^+] following the protocols in Cochilla et al. (4). Forskolin was applied in the presence of IBMX (1 mM). All drugs were prepared in low [K^+] solutions, and all incubations were performed at 37°C.

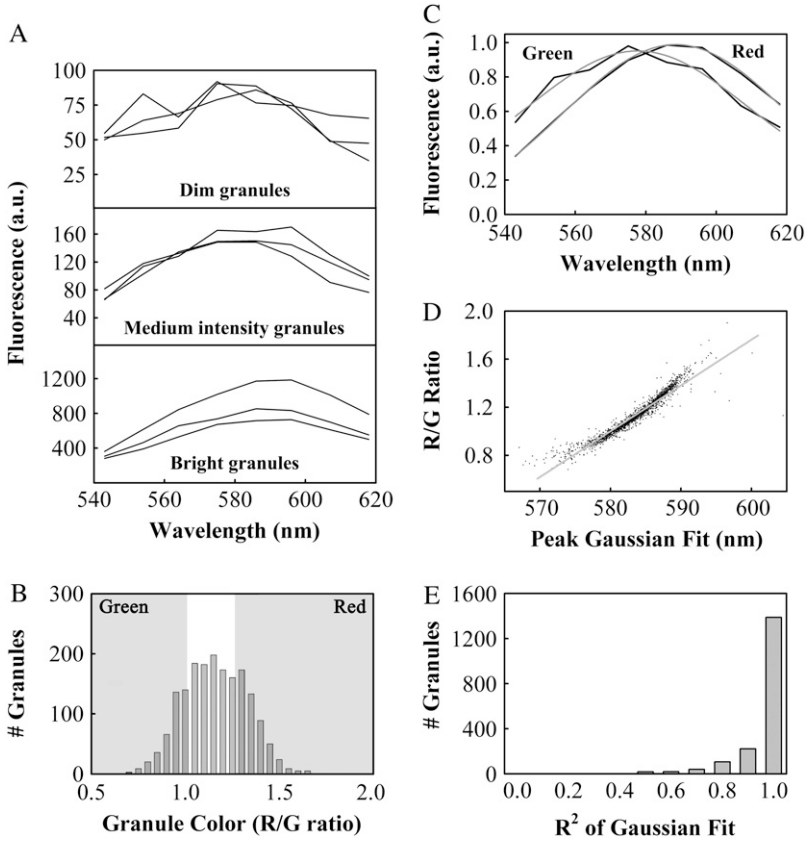

FIGURE 3 Average spectra can be obtained for green and red granules. (*A*) We recorded spectra of individual granules from lactotrophs. Three example spectra each of dim granules (*top panel*), medium intensity (*middle*), and bright granules (*bottom*) are shown. Note the different *y* axis scales for plots of dim, medium intensity, and bright granules. (*B*) A histogram of granule color (R/G values) was normally distributed around a modal value of 1.16. We identified the 400 greenest (R/G ratio <1) and 400 reddest granules (R/G ratio >1.27), as shown in the shaded panels ($n = 1798$ granules, 18 cells, three preparations). (*C*) Using the granules identified in (*B*) we obtained average spectra for green granules and red granules. The average green and red spectra had emission peaks of 578 and 588 nm, respectively, as determined by Gaussian fits (shown in *gray*). (*D*) We fit Gaussian curves to individual spectra of all 1798 granules. We show a scatterplot of R/G ratio as a function of the center of the Gaussian peak. We fit the scatterplot using linear regression, which yielded the equation $R/G = y_0 + m \times P$, with $y_0 = -21.09$ and $m = 0.0381$, resulting in $R^2 = 0.92$. *P* represents the peak wavelength as reported by the Gaussian fit for each granule. (*E*) A histogram of the square of the correlation coefficients (R^2) for Gaussian fits to spectra of all 1798 granules. Almost 90% of the granule spectra could be fit with R^2 values of 0.8 or greater.

RESULTS

Spectra of red and green granules show up to a 25 nm emission shift

To determine the nature of the color shifts observed in FM1-43-stained lactotrophs (Fig. 1), we obtained fluorescence spectra of individual granules using the Zeiss Meta attachment. We stained cells with our standard loading protocol (see Materials and Methods) and recorded spectra from 1798 granules (18 cells, three preparations). In Fig. 3 *A* we show three example spectra each of dim, medium intensity, and bright granules. We selected the spectra of 3 dim granules randomly from the 200 dimmest granules out of 1798, and the spectra of 3 bright granules from the 200 brightest. For the medium intensity spectra we randomly selected 3 out of the 200 granules with intensities in the middle of the range, meaning that there were 799 granules dimmer and 799 granules brighter than this 200. To quantify the color of each granule we defined an R/G as the summed intensity of the emission spectra for the four reddest meta channels (R), divided by the summed intensity of the four greenest channels (G). Fig. 3 *B* shows the distribution of R/G values for 1798 granules from 18 cells. The histogram is normally distributed, not bimodal, meaning that the granules within a cell showed a continuous range of colors. We averaged the spectra of the 400 greenest ($Green_{R/G} < 1$) and 400 reddest ($Red_{R/G} > 1.27$) granules (Fig. 3 *C*) to obtain representative spectra of green and red granules with a good signal/noise ratio. We fit these average spectra to Gaussian functions, shown in gray, which reported emission peaks of 578 and 588 nm. If we averaged the 50 greenest and 50 reddest granules, we obtained spectra with peaks at 573 and 591 nm.

In addition to quantifying color with an R/G ratio, we also fit the spectra of individual granules to Gaussian functions. Fig. 3 *D* shows a scatterplot of R/G ratio as a function of the peak wavelength determined by Gaussian fits for all 1798 granule spectra. Fig. 3 *D* also shows a linear fit to the scatterplot with good correlation ($R^2 = 0.92$). Although the average green and red spectra showed a shift of 10 nm (Fig. 3 *C*), Fig. 3 *D* reported the reddest granules were shifted from the greenest granules by ~25 nm (from 570 to 595 nm). The linearity of the scatterplot suggested that the R/G ratio and the Gaussian fit reported granule color equally well. To evaluate the reliability of the Gaussian fits we relied on correlation coefficients. In Fig. 3 *E* we show a histogram of the square of the correlation coefficients (R^2) for Gaussian fits to all 1798 spectra. Fewer than 11% (190 out of 1798) of the Gaussian fits had R^2 values <0.8, and <5% (85 out of 1798) had $R^2 <$ 0.7. We observed an abrupt drop-off in R^2 for dim granules; however, we determined that granules with poorly fitting spectra ($R^2 < 0.8$) did not skew the color distribution that we measured for all 1798 granules (Fig. S3).

The linear fit in Fig. 3 *D* suggested that the R/G ratio faithfully reflected the peak wavelength reported by Gaussian fits, and we did not find a substantial difference between the two analysis methods. Quantifying color using the R/G ratio has the advantage of utilizing the raw intensity data, without introducing ambiguities due to poor fits. We therefore used the R/G ratio to quantify granule color for the rest of the article (see Figs. 4–8). Fig. 3 *D* conveniently allows any R/G ratio to be converted into an emission peak wavelength.

Granule size was larger than predicted from electron micrographs

During the majority of our analysis, we monitored granule size in 3D in units of pixels. We could not directly convert 3D pixels into a unit of volume (i.e., nm^3) because of the difference in lateral resolution (~350 nm) and *z*-resolution (~1 μm). To determine the size of FM1-43-stained granules in units of nanometers, we measured the number of two-dimensional (2D) pixels in the confocal section in which the granule was largest. This should approximate the equatorial plane of the granule, and the number of pixels in 2D should be proportional to the square of the granule radius. We found a mean granule diameter of 770 nm, with a positively skewed distribution due to an optical limit of 350 nm (Fig. S4). Assuming a normal distribution, the mean granule diameter is equal to the modal value of 700 nm. Our spot picking algorithm reported granule diameters ~20% larger than if measured by hand. With these facts taken together, we predict a mean granule diameter of 560 nm. The diameter of granule cores in lactotrophs taken from male rats has been measured from electron micrographs to be 320 nm (3).

Granule color was correlated with granule fluorescence intensity

For cells stained with our standard protocol, we determined whether granule color and fluorescence intensity were correlated. Fig. 4 *A* shows a scatterplot of granule color (R/G value) versus granule average fluorescence intensity for the same data we presented in Fig. 3. The R/G ratio rises with increasing intensity, up to a maximum value. The data show a large amount of scatter, especially at dim values, which made it difficult to fit to an exponential function. To reduce the amount of scatter, we binned the data into groups of 100 granules, based upon granule intensity (we binned the dimmest 100 granules into the first bin, the next dimmest 100 granules into the second, and so on). We then plotted the average R/G values versus average granule intensity for each bin (Fig. 4 *B*). The binned data could be fit to an exponential rise-to-max function with good correlation (*solid line*, $R^2 = 0.94$).

The data point of lowest intensity does not fall on the exponential fit and has the largest standard error, suggesting that we may have measured the color of the dimmest granules less accurately than bright granules. This is consistent with the fact that spectra that could not be fit well with Gaussian functions ($R^2 < 0.8$) were from low intensity granules (Fig. 3 *E*, Fig. S3). However, we determined that the dimmest

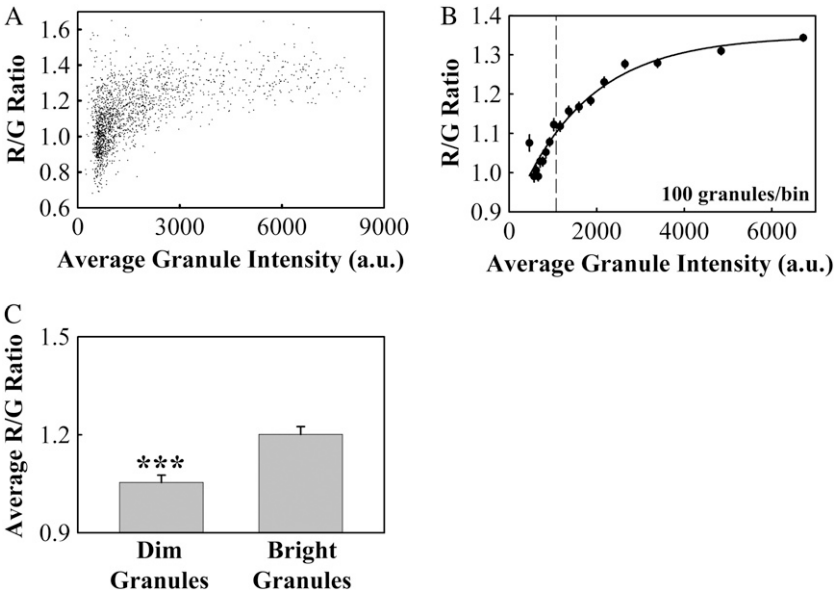

FIGURE 4 Granule color is correlated with granule average fluorescence intensity. (*A*) A scatterplot of R/G ratio versus granule fluorescence intensity for the same data shown in Fig. 3. (*B*) Binned R/G value as a function of binned fluorescence intensity (*filled circles*, error bars represent standard error). The solid line shows an exponential fit to the binned data of the form $R/G = y_0 + a(1 - \exp^{(-bI)})$, with $y_0 = 0.8766$, $a = 0.4714$, and $b = 0.0006$, resulting in $R^2 = 0.94$. I represents the binned granule fluorescence intensity. The dashed line marks the intensity that divides the granules into two groups, the 799 dimmest and 799 brightest. (*C*) We divided granules into two groups, the 50% dimmest and 50% brightest (*dashed line* in Fig. 4 *B*) and determined the average R/G value for each group. Average R/G values (±SE) were 1.20 ± 0.02 for bright granules and 1.05 ± 0.02 for dim granules. Asterisks denote a significant difference ($p < 0.001$, $n = 1798$ granules, 18 cells, three preparations).

granules did not significantly skew the color distribution we measured for all granules (Fig. S3).

To determine if the color of dim granules differed significantly from that of bright granules, we averaged the R/G values for the dimmest 50% and the brightest 50% of all granules (*dashed line* in Fig. 4 *B*). We found that the R/G value of the brightest granules was significantly larger than that of the dimmest granules, meaning the brightest granules appeared significantly redder (Fig. 4 *C*, $p < 0.001$).

Granule color shifted to the red with increasing dye concentration

The observation that granule color was correlated with granule fluorescence intensity suggested that different dye concentrations could be responsible for the variations in granule color. We attempted to induce color shifts by varying the concentration of FM dye that we stained granules with. Fig. 5 *A* shows histograms of R/G values obtained for lactotroph granules loaded with (in μM) 1, 3, 10, and 30 FM1-43. It is clear that the distribution of R/G values shifts to higher values (more red) with increasing FM1-43 concentration. If we arbitrarily define green and red granules using the same R/G values as for Fig. 3 *C* ($Green_{R/G} < 1$, $Red_{R/G} > 1.27$), we see that the number of red granules increased and the number of green granules decreased with increasing FM1-43 concentration, whereas the total number of stained granules remained approximately constant (Fig. 5 *B*). The granule average fluorescence intensity increased with increasing FM1-43 concentration; however, the measured intensity depended nonlinearly on the FM1-43 concentration, indicating quenching of FM1-43 in granules at higher concentrations (Fig. 5 *C*). The average granule size remained constant with increasing FM1-43 concentration, as expected (Fig. 5 *D*).

We determined if FM1-43 underwent a similar concentration-dependent red shift in solution by measuring the emission spectra of FM1-43 bound to reconstituted (egg PC) vesicles or to dissolved PRL. The quantum yield of FM1-43 in solution increased to similar extents upon binding to egg PC vesicles or PRL (Fig. S2, *A–D*). Increasing FM1-43 concentration from 1 to 30 μM caused the emission peak to shift from 590 to 603 nm when bound to vesicles and from 592 to 602 nm when bound to PRL, as determined by Gaussian fits to the spectra (Fig. S2, *E* and *F*, and Table S1), as well as a quenching effect that reduced the emission intensity at the highest FM dye concentrations (data not shown). The concentration-dependent red shift of FM1-43 bound to PC vesicles in solution has been previously reported, although mechanisms of the red shift were not investigated (10).

Granule color could be shifted to the green by partial photobleaching

To confirm that granule color was related to dye concentration, we performed a photobleaching test, predicting that reducing dye concentration by photobleaching should green shift granule color. We imaged lactotrophs loaded with our standard protocol (100 mM KCl, 4 μM FM1-43) in the equatorial plane, photobleached with 100% laser intensity for a single pass, and imaged again. Granule fluorescence intensity was reduced by approximately half for all granules. The spectra averaged over all granules shows a slight but observable shift to the green after photobleaching (Fig. 6 *A*). Following the method used in Fig. 4 *A*, we binned the granules based upon granule fluorescence intensity (10 granules per bin). Fig. 6 *B* shows data points representing binned R/G ratio versus granule intensity for granules before photobleaching connected to data points representing the same

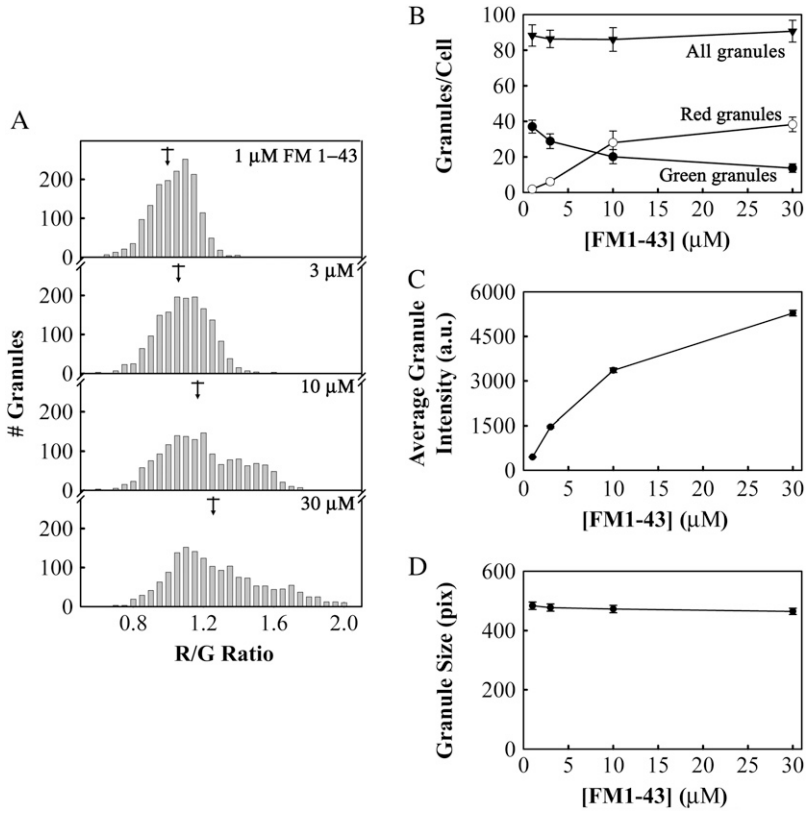

FIGURE 5 Granule color shifted to the red with increasing FM1-43 concentration. (*A*) Lactotrophs were stimulated with 100 mM KCl in varying concentrations of FM dye. The mean R/G ratio (±SE) for 1, 3, 10, and 30 μM FM1-43 were 1.011 ± 0.003, 1.062 ± 0.004, 1.166 ± 0.006, and 1.261 ± 0.007 (marked by *arrows*). (*B*) The total number of granules (*triangles*), the number of red granules (*open circles*), and the number of green granules per cell (*filled circles*) as a function of FM1-43 concentration. The total number of granules includes red, yellow, and green granules, as defined in Fig. 3 *B*. (*C*) Granule average fluorescence intensity (a.u.) as a function of FM1-43 concentration. (*D*) Granule size, in pixels, as a function of FM1-43 concentration. All error bars are standard error (n = 1500–1800 granules, 18 cells, three preparations for each FM1-43 concentration).

granules after photobleaching (*filled circles* connected by *thin lines*).

On the same axes we also plot the exponential fit from Fig. 4 *B* (R/G ratio versus intensity), which predicts reasonably well the color changes of granules we observed upon photobleaching. This suggests that we could change granule color by modulating the granule intensity, and we assume granule intensity proportional to FM1-43 concentration. The average R/G value showed a significant decrease after photobleaching, as granules shifted to the green have smaller R/G values ($p < 0.001$, Fig. 6 *C*). Photobleaching decreased the average fluorescence intensity of all granules by 1925 arbitrary units (a.u.). The exponential fit from Fig. 4 *B* predicts $\Delta R/G = -0.08$ for this decrease in intensity, and we measured an average (±standard error) $\Delta R/G = -0.08 \pm 0.03$.

Granule color depended on stimulation intensity

After observing that granule color depended upon dye concentration, we determined if increasing stimulation intensity would cause granules to take up more dye during exocytosis, resulting in a red shift of granule fluorescence. Fig. 7 *A* shows histograms of R/G values for lactotrophs stimulated with (in mM) 5, 25, 50, 75, and 100 KCl in the presence of 4 μM FM1-43. Fig. 7 *B* shows the number of red granules and green granules and total number of granules per cell as a function of KCl concentration ($Green_{R/G} < 1$, $Red_{R/G} > 1.27$). The total number of granules increased asymptotically with increasing KCl concentration, appearing to reach a maximum near 100 granules per cell. The number of green granules increased up to a maximum at 50 mM KCl and then decreased, whereas the number of red granules increased most at KCl concentrations above 50 mM. The granule average fluorescence intensity (Fig. 7 *C*) increased from 1120 to 1400 a.u.—with KCl concentrations increasing from 5 to 25 mM—stayed fairly constant up to 50 mM KCl, and then increased again to 1800 a.u. with 75 and 100 mM KCl.

The granule size (Fig. 7 *D*) displayed a similar pattern, increasing from 360 to 400 pixels—with KCl increasing from 5 to 25 mM—staying constant with KCl up to 50 mM, and then increasing again to 450 and 500 pixels with KCl concentrations of 75 and 100 mM, respectively. In summary, KCl concentrations of 25 and 50 mM appeared to elicit exocytosis of smaller, less brightly staining granules than concentrations of 75 and 100 mM KCl. The lowest KCl concentration (5 mM) barely elicited exocytosis of any granules at all (Fig. 7 *B*), demonstrating that we are not monitoring constitutive uptake of FM dye.

The stimulation-dependent red shift was not due to increased staining rates or increased compound exocytosis

Why would granules take up more dye when stimulated more intensely? One possible answer concerns the mode of fusion.

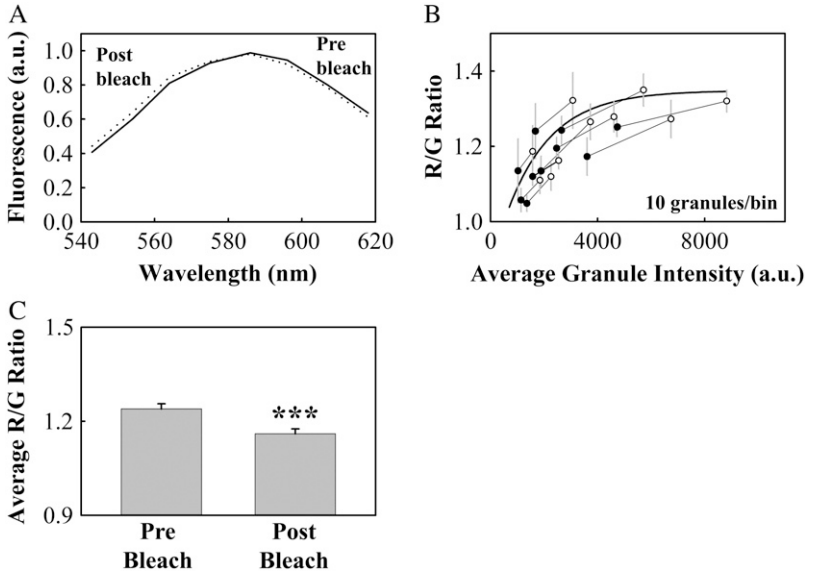

FIGURE 6 Granule color could be shifted to the green by partial photobleaching of FM1-43. (*A*) Average spectra of FM1-43-stained granules from a single confocal plane (equatorial) of a cell before (*solid line*) and after (*dotted line*) photobleaching. (*B*) Binned R/G ratio as a function of intensity for granules before and after photobleaching, along with the exponential fit from Fig. 4 *A* (*thick line*). Bins of the same granules before (*open circles*) and after (*filled circles*) photobleaching are shown connected by thin lines. (*C*) The average (±SE) R/G value before photobleaching was 1.24 ± 0.02 and after photobleaching was 1.16 ± 0.02. Asterisks denote a significant difference ($p < 0.001$, $n = 103$ granules, five cells, one preparation). All error bars represent standard error.

For example, it is possible that with milder stimulation the access of FM dye to granule cores is restricted, limiting the rate of dye entry. If more intense stimulation allowed unrestricted entry of FM dye, granules might take up more dye and be red shifted. To test this, we measured the kinetics of granule staining during light stimulation (50 mM KCl) and heavy stimulation (100 mM KCl). We compared these two stimulation intensities because we observed the maximum number of green granules in cells stimulated with 50 mM KCl and the maximum number of red granules in cells stimulated with 100 mM KCl (Fig. 7 *B*). Fig. 8 *A* shows example traces from exocytic granules, obtained by imaging at relatively high rates (4 Hz) during stimulation in the presence of 4 μM FM1-43.

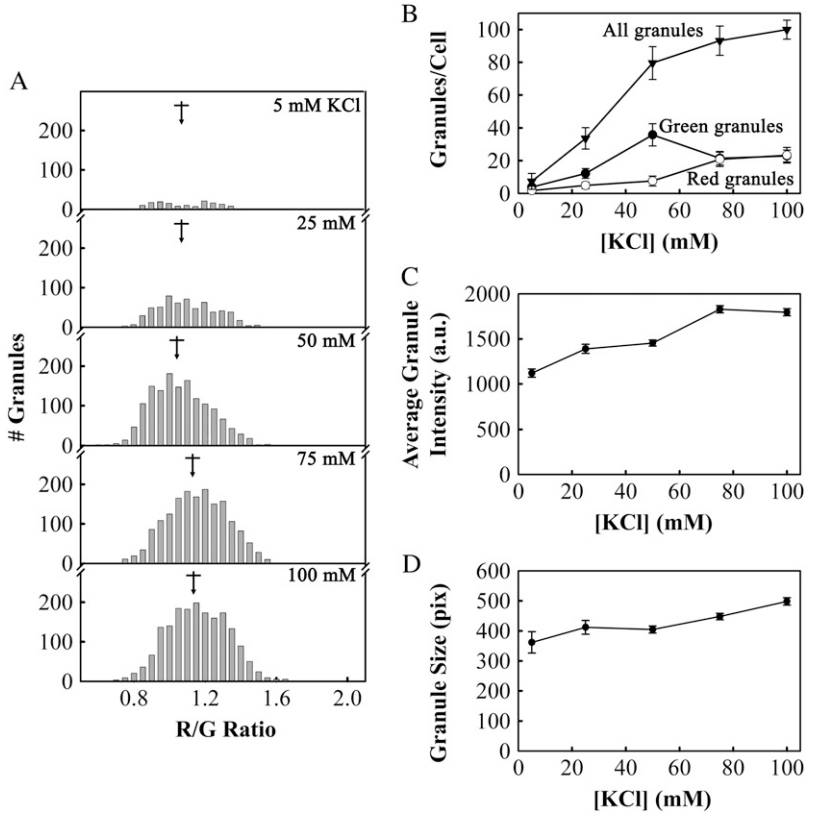

FIGURE 7 Granule color depended upon stimulation intensity. (*A*) We measured the spectra of granules in lactotrophs stimulated with 5, 25, 50, 75, and 100 mM KCl in the presence of FM1-43 and plotted the resulting color distributions. The mean R/G values for each KCl concentration (±SE) in increasing order were 1.06 ± 0.01, 1.078 ± 0.007, 1.038 ± 0.004, 1.131 ± 0. 004, and 1.135 ± 0. 004 (marked by *arrows*). (*B*) The total number of granules (*triangles*), the number of green granules (*filled circles*), and the number of red granules per cell (*open circles*) as a function of KCl concentration. The total number of granules includes red, yellow, and green granules, as defined in Fig. 3 *B*. (*C*) Granule average fluorescence intensity and (*D*) granule size as a function of increasing KCl concentration. All error bars represent standard error ($n = 153$, 604, 1431, 1677, and 1798 granules for each KCl concentration, 18 cells, three preparations for each KCl concentration).

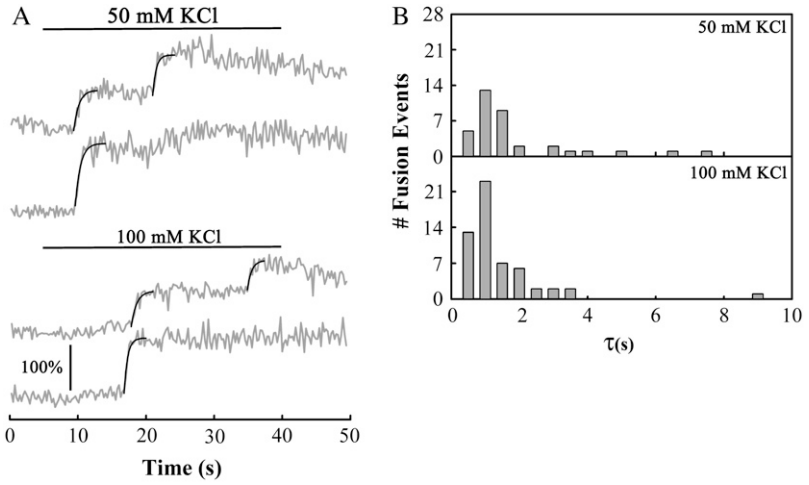

FIGURE 8 Kinetics of FM1-43 staining of granules was independent of stimulation intensity. (*A*) Example fluorescence traces of cells stimulated with 50 mM or 100 mM KCl, applied during times indicated by the solid lines (see Movie S3). The vertical scale bar indicates a 100% increase in fluorescence above the level of the membrane stain; all traces are on the same fluorescence intensity scale. Smooth lines indicate exponential fits to fluorescence rise times. (*B*) Histograms of rise times for fusion events in cells stimulated with 50 mM or 100 mM KCl. The average rise time (±SE) was 1.7 ± 0.3 s for 50 mM KCl and 1.1 ±0.2 s for 100 mM KCl ($p > 0.2$, $n = 37$, and 56 events for 50 mM and 100 mM stimulation, respectively, seven cells each, one preparation).

Multiple steps are visible in two of the example traces, reflecting compound exocytosis, which is common in lactotrophs (3). The black lines are best fit curves to a rising exponential of the form $I(t) = I_0 + I_\Delta(1 - e^{-t/\tau})$, where t is time (s), I is the fluorescence intensity, I_0 is the intensity before the abrupt increase due to exocytosis, I_Δ is the magnitude of the intensity increase, and τ is the exponential time constant. Fig. 8 *B* shows histograms of time constants (τ) determined from the exponential fits for 50 and 100 mM KCl traces. The average time constant (±SE) was 1.7 ± 0.3 s for 50 mM KCl and 1.1 ± 0.2 s for 100 mM KCl; however, the difference between the two time constants was not statistically significant ($p > 0.2$). Furthermore, each average rise time was considerably shorter than the 10–15 min endocytic timescale for lactotroph cells (3). This suggests that a restricted rate of dye uptake was not responsible for the increased number of green granules in lactotrophs stimulated with 50 mM KCl.

We also attempted to determine whether compound exocytosis was responsible for causing red granules (data not shown). Using our standard stimulation protocol, we stained cells in the presence of forskolin or PMA, both of which increase the amount of compound exocytosis in lactotrophs (4). PMA increased the total number of granules per cell, which has been previously observed; however, neither drug caused a significant change in the proportion of red to green granules per cell. Using 25 mM KCl to stimulate cells in the presence of PMA also did not change the proportion of red to green granules, compared to stimulation with 25 mM KCl alone.

DISCUSSION

The FM1-43-stained spots identified in our lactotroph cells appear to be PRL positive granules. Lactotrophs did not take up a significant amount of FM dye at rest (Fig. 7 *B*). Furthermore, the facts that FM1-43 is bound by PRL and stains granule cores brightly help to differentiate PRL positive granules from FM1-43 staining of other cellular structures. Bauer et al. (11) have demonstrated that endocytosed lactotroph granules are sent to early endosomes or the endosomal recycling compartment but do not colocalize with degradative lysosomes or the trans-Golgi. They also found that recycled granules were preferentially exocytosed upon a second stimulus. This suggests that the FM dye labeled structures we imaged were PRL positive granular structures, which could be released again upon a second stimulus. The average diameter of the granules we measured by fluorescence was 1.75 times larger than the diameter of granule cores measured by electron micrograph studies (3). Bauer et al. (11) also noted that granules labeled with fluorescent antibodies increased in size 20–80 min after endocytosis, and they postulated that granules undergo homotypic fusion to become ready for a second round of exocytosis. Alternatively, granules that had undergone compound exocytosis could appear as one spherical shape in our fluorescence measurements, explaining their large size. Approximately five granules would need to fuse together for an increase in diameter of 1.75 times.

FM1-43 has been previously observed to fluoresce in different colors, depending upon the microscopic environment of the dye. For example, in frog nerve muscle preparations, FM1-43 in synaptic vesicles is yellow, in myelin FM1-43 is green, and in Schwann cell endosomes FM1-43 is orange (12). Jin et al. (13) have demonstrated that the styryl dye di-4-ANEPPDHQ, which is structurally similar to FM1-43, undergoes a 30 nm emission blue shift with increasing cholesterol content in vesicles. The authors hypothesized that increased rigidity of the membrane environment, which reduces the magnitude of the observed Stokes shift, caused the color shift. The environmental sensitivity of FM1-43 fluorescence raises the question of whether FM1-43 fluoresces with a different color when bound to granule membrane as opposed to granule cores.

One could imagine, for example, that green granules have more FM dye bound to granule membranes, whereas red granules have more FM dye bound to the granule core. However, FM1-43 fluoresces with the same peak wavelength

when bound to vesicles in solution as when bound to PRL (Fig. S2). Furthermore, Angleson et al. demonstrated that lactotroph granule cores bind ~13 times as much FM dye as the granule membrane (3). Because <8% of our fluorescence signal originated from membrane-bound FM1-43, FM1-43 bound to granule cores dominated the color of fluorescence we observed. The color differences between FM1-43-stained lactotroph granules appear to be due to different dye concentrations within the granules. The color of the granules was correlated with the average brightness of the granules (which is proportional to the dye concentration), and we could reproduce similar red shifts by increasing the external concentration of FM dye loaded into granules. Furthermore, granules could be green shifted by partial photobleaching, although our analysis of the photobleaching experiment assumed that red-shifted and green-shifted FM1-43 bleach with equal efficiency and that bleaching does not create fluorescent byproducts with shifted emission spectra.

For the most part, our experiments examined a system in equilibrium. The slow endocytic process allowed sufficient time for FM1-43 in solution to equilibrate with FM1-43 bound to granules. Monitoring changes in granule color during the exocytic event could provide verification of our hypothesis: as granules took up more FM dye, the granule color should shift to the red. However, the integration time of the Zeiss Meta detector necessary to measure spectra of individual granules combined with the rapid staining time of granules (1–2 s, Fig. 8) precludes this test at the current time. Monitoring color changes of preloaded granules during release of FM dye (during a second round of stimulation) would also provide an interesting test, but we expect release also to occur with a rapid time course.

Two possible causes of a concentration-dependent color shift are an ''inner filter effect'' and physical interactions between dye molecules. At sufficiently high concentrations an inner filter effect can cause a red shift. When a fluorophore has a small stokes shift, photons emitted at the short wavelength side of the emission spectrum can be reabsorbed, which results in a loss of detected fluorescence in the overlap region and red shifting of the emission peak (14). We can predict the extent of photon reabsorption, A, from Beer's law: $A = \varepsilon bc$, where ε is the (wavelength-dependent) extinction coefficient, b is the path length of photons traveling through neighboring dye molecules, and c is the concentration of dye molecules. We express A in units of optical density (OD). Assuming $\varepsilon = 10{,}000\ \mathrm{cm^{-1}M^{-1}}$ where the excitation and emission bands of FM1-43 overlap, we can calculate the approximate absorbance of emitted fluorescence for FM1-43 bound to vesicles or PRL in solution (Fig. S2). We used a 1 cm cuvette for solution experiments, so $b = 1$ cm and $A =$ 0.01, 0.03, 0.1, and 0.3 for solutions of (in μM) 1, 3, 10, and 30 FM1-43. Inner filter effects are considered to occur at an OD above 0.05 (14), which suggests that inner filter effects could have caused the concentration-dependent red shift of FM1-43 in solution, at least in part.

We do not know the concentration of FM1-43 within lactotroph granules. However, due to the small path length of granules (compared to a 1 cm cuvette), reabsorption of emitted photons would not occur unless granules contained a very high concentration of FM1-43. Assuming $b = 500$ nm for granules, we can estimate that granules would need to contain ~100 mM FM1-43 to reach an OD of 0.05. This would constitute a 10^4 increase of FM dye concentration as compared to a 10 μM solution. Using fluorescence and calorimetry techniques, Schote and Seelig have measured the partition equilibrium of FM1-43 binding to neutral and negatively charged PC vesicles (15). Betz and colleagues have measured the number of dye molecules taken up by synaptic vesicles from a solution of 4 μM FM1-43. By measuring fluorescence released into solution upon stimulation of a previously labeled nerve terminal, the authors estimated that each synaptic vesicle contained 383 FM1-43 molecules (16).

If we use the equilibrium binding constant measured by Schote and Seelig, we predict a synaptic vesicle to take up between 200 and 400 FM1-43 molecules, in good agreement with the measured value. The range in the prediction depends on whether the inner leaflet of the synaptic vesicle is neutral or negatively charged. For a 560 nm granule in equilibrium with a solution of 10 μM FM1-43, we calculate the granule membrane would contain between 1 and 2×10^5 FM1-43 molecules, depending on whether the granule membrane more closely resembled a neutral vesicle or a negatively charged vesicle. We also know that the granule core has the capacity to bind 13× as much FM1-43 as the granule membrane (3), meaning that a 560 nm granule should contain, in total, between 1.4 and 2.8×10^6 molecules of FM1-43. This translates into a granule concentration between 25 and 50 mM. For comparison, it would be interesting to know the concentration of PRL within granule cores. As far as we know, this has not been determined; however the concentration of insulin within secretory granules has been measured to be 42 mM (17). These calculations suggest that inner filter effects could be at least a partial explanation for the concentration-dependent color shifts we have observed in lactotroph granules.

Physical interactions of FM dyes could also cause a concentration-dependent color shift. Amphiphilic styryl dyes, similar in structure to FM 1-43, have been previously shown to undergo concentration-dependent red shifts in fluorescence. Turshatov et al. (18) demonstrated that styryl dyes in Langmuir-Blodgett films underwent a 65 nm red shift in fluorescence when they reduced the molecular area in the film by a factor of four. The authors suggest that the red shift was due to dimerization of the dye molecules. Other amphiphilic styryl dyes in crystals and monolayer assemblies have been found to have fluorescence red shifted by ~75 nm relative to their fluorescence in solution, due to formation of excited state dimers (excimers) (19). dipyrromethene boron difluoride (BODIPY)-labeled lipids are also known to form excimers

with a 100 nm red shift, which has been used to selectively monitor cell organelles in which the lipid is concentrated (20). In addition to excimer emission, the wavelength of monomer emission of BODIPY lipids in Langmuir monolayers increases linearly with increasing dye concentration, shifting 20 nm to the red over a 200-fold increase in concentration (21). The authors suggest that the 20 nm red shift could reflect electronic interactions among nonaggregated fluorophores (21). This is similar in amplitude to the red shift that FM 1-43 undergoes in granules, suggesting that similar electronic interactions could be responsible for altering the color of FM1-43 fluorescence as well.

We have observed that granule color shifts to the red with increasing stimulation intensity (Fig. 7). We consider three mechanisms that could cause lactotroph granules to bind more FM dye with increased stimulation intensity.

1. Increased rate of dye uptake: Either the diameter of the fusion pore or the duration of the fusion time increases with increased stimulation intensity, allowing more FM dye to enter granule cores. Zorec and colleagues (22) have recently demonstrated that lactotroph granules exocytose with a ''flickering'' fusion pore and that stimulation with 100 mM KCl increased the fusion pore conductance more than granules fusing spontaneously. In lactotrophs stimulated with 100 mM KCl, exocytosing granules stain rapidly with FM dye and remain fused to the plasma membrane for ~15 min, allowing sufficient time for FM dye to saturate the granule core (3). It is possible that at lower stimulation intensities access to granule cores is restricted, through either a restricted fusion pore or a shorter ''flicker'' time, causing granules to take up less FM dye. Lactotrophs stimulated with 50 mM KCl showed the largest proportion of green granules (Fig. 7 *B*). However, granules stained with FM dye just as rapidly whether lactotrophs were stimulated with 50 or 100 mM KCl, suggesting that decreased access to granule cores is not responsible for the higher proportion of green granules at 50 mM KCl. Zorec and colleagues (23) have also reported that lactotroph granules load with FM dye rapidly (in ~10 s) when stimulated with 100 mM KCl.
2. Compound exocytosis: The inner filter effect is path length dependent; therefore FM dye staining multiple granule cores fused together could suffer a more extensive inner filter effect. The amount and magnitude of compound fusion events increases with increasing KCl concentration (4). However, we did not see an increase in the proportion of red granules when we promoted compound exocytosis using either PMA or forskolin.
3. Granule structural differences: Some granules have more dense cores than others, providing more FM1-43 binding sites. The denser granules also require a stronger stimulus to exocytose. In a series of articles utilizing quantitative electron microscope autoradiography (6,7), Farquhar and colleagues demonstrated that as lactotroph granules age they increase in size through homotypic fusion and their cores become more dense. They also demonstrated that younger granules release preferentially under basal conditions, whereas older granules require stimulation to release. This may be a general trait in neuroendocrine cells: Chow and colleagues (24) have demonstrated that younger granules release preferentially with mild stimulation in chromaffin cells. We found that stimulation intensity was correlated both with granule average fluorescence intensity and granule size (Fig. 7, *C* and *D*). This suggests that there is a hierarchy in release probability in which larger, denser granules require more intense stimulation to be released. Denser granules are also able to take up more FM dye and thus appear redder. As KCl concentration increases from 5 to 50 mM, small, less dense granules exocytose, causing an increase in the number of green granules. Above 50 mM KCl the total number of exocytosed granules continues to increase. However, the size and density of the exocytosed granules also increases, causing a larger proportion of red to green granules (Fig. 7 *B*). Mechanism (iii) appears to most satisfactorily explain the stimulation-dependent color shifts we have observed in FM1-43-stained granules.

This work serves as a cautionary note for studying FM dye fluorescence. Slight color variations due to increased FM dye concentration could be misinterpreted as a decrease in fluorescence if monitored at the wrong wavelength. Furthermore, concentration-dependent color shifts could be useful for monitoring aggregation of fluorescent labels below the optical limit. In this study, concentration-dependent color shifts suggest that some granules can more tightly pack FM dye molecules due to more dense cores. If we had only monitored total fluorescence intensity, we may have interpreted our results as increased granule size and would have missed the information suggesting an increase in core density.

Homo-FRET (fluorescence resonance energy transfer) is another technique utilizing a single fluorescent label that has been used as a tool for monitoring aggregation states of proteins and measuring the size of lipid rafts in vivo (25,26). The advantages of using only a single fluorescent tag (as opposed to hetero-FRET techniques) are the simplification of the tagging protocol and the fact that every dye molecule can act as either an energy donor or acceptor. The extent of aggregation in homo-FRET experiments is normally determined by measuring the anisotropy of the fluorescent tags, which will decrease as the amount of energy transfer increases. Our study presents a complementary technique in which the relative concentration of a fluorophore is monitored through a color shift of the emitted fluorescence.

SUPPLEMENTARY MATERIAL

To view all of the supplemental files associated with this article, visit www.biophysj.org.

We acknowledge Michael Gaffield and Dr. Leah Sheridan for extensive helpful discussions, Steve Fadul for technical assistance, and Dr. Nicholas Barry for microscopy assistance and providing the standard spectrum of R6G.

This work was funded by research grants from the National Institutes of Health National Institute of Neurological Disorders and Stroke (W.J.B.) and a fellowship from National Institutes of Health (J.M.J.).

REFERENCES

1. Freeman, M. E., B. Kanyicska, A. Lerant, and G. Nagy. 2000. Prolactin: structure, function, and regulation of secretion. *Physiol. Rev.* 80:1523–1631.
2. Cochilla, A. J., J. K. Angleson, and W. J. Betz. 1999. Monitoring secretory membrane with FM1-43 fluorescence. *Annu. Rev. Neurosci.* 22:1–10.
3. Angleson, J. K., A. J. Cochilla, G. Kilic, I. Nussinovitch, and W. J. Betz. 1999. Regulation of dense core release from neuroendocrine cells revealed by imaging single exocytic events. *Nat. Neurosci.* 2:440–446.
4. Cochilla, A. J., J. K. Angleson, and W. J. Betz. 2000. Differential regulation of granule-to-granule and granule-to-plasma membrane fusion during secretion from rat pituitary lactotrophs. *J. Cell Biol.* 150:839–848.
5. Petzold, A., and L. T. Sharpe. 1998. Hue memory and discrimination in young children. *Vision Res.* 38:3759–3772.
6. Farquhar, M. G., J. J. Reid, and L. W. Daniell. 1978. Intracellular-transport and packaging of prolactin-quantitative electron-microscope auto-radiographic study of mammotrophs dissociated from rat pituitaries. *Endocrinology.* 102:296–311.
7. Walker, A. M., M. G. Farquhar, and B. Peng. 1980. Preferential release of newly synthesized prolactin granules is the result of functional-heterogeneity among mammotrophs. *Endocrinology.* 107:1095–1104.
8. Johnson, J. M., and W. J. Betz. 2006. Fluorescent membrane marker FM 1-43 undergoes a spectral shift in lactotroph granules. 2006 Biophysical Society Meeting Abstracts. *Biophys. J.* 90:2305. (Abstr.).
9. Johnson, J. M., T. Ha, S. Chu, and S. G. Boxer. 2002. Early steps of supported bilayer formation probed by single vesicle fluorescence assays. *Biophys. J.* 83:3371–3379.
10. Richards, D. A., J. H. Bai, and E. R. Chapman. 2005. Two modes of exocytosis at hippocampal synapses revealed by rate of FM 1-43 efflux from individual vesicles. *J. Cell Biol.* 168:929–939.
11. Bauer, R. A., R. L. Overlease, J. L. Lieber, and J. K. Angleson. 2004. Retention and stimulus-dependent recycling of dense core vesicle content in neuroendocrine cells. *J. Cell Sci.* 117:2193–2202.
12. Betz, W. J., F. Mao, and G. S. Bewick. 1992. Activity-dependent fluorescent staining and destaining of living vertebrate motor nerve terminals. *J. Neurosci.* 12:363–375.
13. Jin, L., A. C. Millard, J. P. Wuskell, X. M. Dong, D. Q. Wu, H. A. Clark, and L. M. Loew. 2006. Characterization and application of a new optical probe for membrane lipid domains. *Biophys. J.* 90:2563–2575.
14. Lakowicz, J. R. 1999. Principles of Fluorescence Spectroscopy. Kluwer Academic/Plenum Publishers, New York.
15. Schote, U., and J. Seelig. 1998. Interaction of the neuronal marker dye FM1–43 with lipid membranes—thermodynamics and lipid ordering. *Biochim Biophys Acta.* 1415:135–146.
16. Henkel, A. W., J. Lubke, and W. J. Betz. 1996. FM1-43 dye ultrastructural localization in and release from frog motor nerve terminals. *Proc. Natl. Acad. Sci. USA.* 93:1918–1923.
17. Hutton, J. C., E. J. Penn, and M. Peshavaria. 1983. Low-molecular-weight constituents of isolated insulin-secretory granules—bivalent-cations, adenine-nucleotides and inorganic-phosphate. *Biochem. J.* 210:297–305.
18. Turshatov, A. A., M. L. Bossi, D. Mobius, S. W. Hell, A. I. Vedernikov, S. P. Gromov, N. A. Lobova, M. V. Alfimov, and S. Y. Zaitsev. 2005. Spectroscopic properties of an amphiphilic styryl pyridinium dye in Langmuir-Blodgett films. *Thin Solid Films.* 476: 336–339.
19. Quina, F. H., and D. G. Whitten. 1977. Photochemical reactions in organized monolayer assemblies. 4. Photodimerization, photoisomerization, and excimer formation with surfactant olefins and dienes in monolayer assemblies, crystals, and micelles. *J. Am. Chem. Soc.* 99:877–883.
20. Pagano, R. E., O. C. Martin, H. C. Kang, and R. P. Haugland. 1991. A novel fluorescent ceramide analog for studying membrane traffic in animal-cells—accumulation at the Golgi-apparatus results in altered spectral properties of the sphingolipid precursor. *J. Cell Biol.* 113: 1267–1279.
21. Dahim, M., N. K. Mizuno, X. M. Li, W. E. Momsen, M. M. Momsen, and H. L. Brockman. 2002. Physical and photophysical characterization of a BODIPY phosphatidylcholine as a membrane probe. *Biophys. J.* 83:1511–1524.
22. Vardjan, N., M. Stenovec, J. Jorgacevski, M. Kreft, and R. Zorec. 2007. Subnanometer fusion pores in spontaneous exocytosis of peptidergic vesicles. *J. Neurosci.* 27:4737–4746.
23. Stenovec, M., I. Poberaj, M. Kreft, and R. Zorec. 2005. Concentration-dependent staining of lactotroph vesicles by FM 4-64. *Biophys. J.* 88:2607–2613.
24. Duncan, R. R., J. Greaves, U. K. Wiegand, I. Matskovich, G. Bodammer, D. K. Apps, M. J. Shipston, and R. H. Chow. 2003. Functional and spatial segregation of secretory vesicle pools according to vesicle age. *Nature.* 422:176–180.
25. Rao, M., and S. Mayor. 2005. Use of Forster's resonance energy transfer microscopy to study lipid rafts. *Biochim. Biophys. Acta.* 1746:221–233.
26. Gautier, I., M. Tramier, C. Durieux, J. Coppey, R. B. Pansu, J. C. Nicolas, K. Kemnitz, and M. Coppey-Moisan. 2001. Homo-FRET microscopy in living cells to measure monomer-dimer transition of GFP-tagged proteins. *Biophys. J.* 80:3000–3008.